# 3D Assembly of Semiconductor and Metal Nanocrystals: Hybrid CdTe/Au Structures with Controlled Content

Vladimir Lesnyak,[†] André Wolf,[†] Aliaksei Dubavik,[†] Lars Borchardt,[§] Sergei V. Voitekhovich,[‡] Nikolai Gaponik,[†] Stefan Kaskel,[§] and Alexander Eychmüller*,[†]

[†]Physical Chemistry, TU Dresden, Bergstr. 66b, 01062 Dresden, Germany

[§]Inorganic Chemistry, TU Dresden, Bergstr. 66, 01062 Dresden, Germany

[‡]Research Institute for Physical Chemical Problems, Belarusian State University, Leningradskaya Str. 14, 220030 Minsk, Belarus

Ⓢ *Supporting Information*

**ABSTRACT:** A 3D metal ion assisted assembly of nanoparticles has been developed. The approach relies on the efficient complexation of cadmium ions and 5-mercaptomethyltetrazole employed as the stabilizer of both colloidal CdTe and Au nanoparticles. It enables in a facile way the formation of hybrid metal-semiconductor 3D structures with controllable and tunable composition in aqueous media. By means of critical point drying, these assemblies form highly porous aerogels. The hybrid architectures obtained are characterized by electron microscopy, nitrogen adsorption, and optical spectroscopy methods.
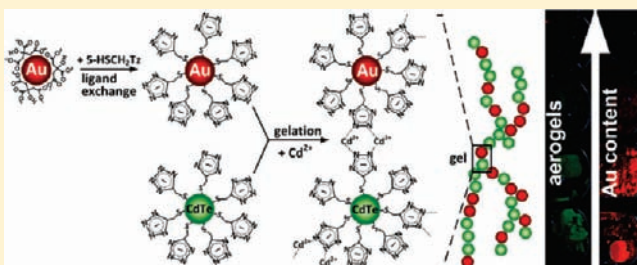
## INTRODUCTION

Various assemblies and self-assemblies of nanocrystalline materials have attracted emerging scientific interest during recent years. Among other constituents, colloidal semiconductor and metal nanocrystals (NCs) are used for the preparation of artificial molecules and solids.[1] To date, the approaches developed for assembling provide options to obtain 1D, 2D, and 3D nanostructures.[2] The creation of such novel architectures using bottom-up approaches allows one to transfer properties of the nanoparticles to the macro-scale, by this bridging the nano- and macro-worlds. At the same time, the interparticle interactions realized in the assembled structures impact on their resulting properties. Interactions occur by means of special linkers or via direct contact between the nanounits. Thus, interlinking gold NCs into three-dimensional assemblies enables one to tune their conductivity from the insulating to the metallic limit retaining the optical properties peculiar to gold in its nanoparticulate form.[3] Recently, attention was attracted by the possibility to create functional gels and aerogels via self-assembly of colloidal NCs[4] or clusters of metal chalcogenides,[5] which may open enormous opportunities for semiconductor technology, catalysis and photocatalysis, optoelectronics and photonics, sorbents and filters. Aerogels are highly porous monoliths, which when assembled from semiconductor NCs preserve their strong light emission while simultaneously exhibiting a structure being beneficial for charge and energy transfer.[4b,c,6] Additionally, nanostructured networks may be formed from noble metals.[7] Those exhibit less than 1/1000th of the density of the respective bulk metals and open avenues to sensoric, catalytic or nanophotonic applications.[7a] Additional opportunities to obtain structures with properties complementary to or different from those being characteristic for the initial building blocks arise if assemblies are made from nanounits of more than one material, e.g. from semiconductor and metal nanoparticles. In this case, the variety of properties of the resulting hybrid composites is greatly extended by the tuning of their respective contents and by this offering new perspectives for their applications.

In this work, we present a new method of a facile and controllable assembly of CdTe and Au NCs employing a recently reported approach.[8] The concept of reversible metal ion-assisted assembly has been successfully applied for the preparation of hybrid metal-semiconductor 3D architectures. The formation of the network occurs owing to the excellent complexing properties of the capping ligand 5-mercaptomethyltetrazole (5-HSCH$_2$Tz) cross-linking the NCs through Cd$^{2+}$ ions. Tuning the ratio semiconductor NCs to metal NCs and the content of the cadmium salt allows an effective control of the level of aggregation of the NCs, of the composition of the assemblies, and consequently of their properties. The hybrid architectures obtained were characterized by means of electron microscopy and optical spectroscopy. The results show a gradual photoluminescence (PL) quenching with increasing gold content in the structure.

## EXPERIMENTAL SECTION

**Synthesis of CdTe/5-HSCH$_2$Tz NCs.** The synthesis of 5-HSCH$_2$Tz as well as the aqueous synthesis of the CdTe NCs capped by this tetrazole have been performed according to ref 8.

**Synthesis of Colloidal Au NCs.** Gold colloid was obtained according to ref 9. Typically, 1 mL of 1% $HAuCl_4$ (10 mg, 2.94 × $10^{-2}$ mmol) water solution was diluted by 90 mL of Milli-Q water in a beaker at room temperature. After 1 min of intensive agitating 1 mL of 1% sodium citrate (10 mg, 3.88 × $10^{-2}$ mmol) was added to the solution. In 1 min intervals 1 mL of freshly prepared 0.075% $NaBH_4$ (0.75 mg, 1.98 × $10^{-2}$ mmol) in 1% sodium citrate solution was injected into the precursor mixture. The color of the resulting gold colloid turned ruby-red. After 1 h, the reaction was completed. The average size of the nanoparticles as determined from TEM measurements is ca. 3 nm.

**Ligand Exchange for Au NCs.** The gold colloid obtained was mixed with 10.2 mg (8.82 × $10^{-2}$ mmol) of 5-$HSCH_2$Tz dissolved in 1 mL of 0.1 M NaOH solution and stirred overnight. The molar ratio of Tz/Au = 3/1. After ligand exchange, the colloidal Au can easily be concentrated by vacuum evaporation. The Au/5-$HSCH_2$Tz nanoparticles were precipitated by the addition of THF (1/2 volume ratio) and separated by centrifugation. The NCs obtained are readily redispersible in water and alcohols.

**Preparation of CdTe, Au and Hybrid CdTe/Au Hydro- And Aerogels.** Two different fractions of CdTe colloid have been used for the gel preparations. One, referred as CdTe-g has average NC diameters of 2 nm and green PL with a maximum centered at appox. 530 nm, the other—CdTe-o contains 3 nm particles and luminesces with a maximum at appox. 600 nm. The concentrations of the reprecipitated CdTe-g, CdTe-o, and Au NCs were 70, 115, and 28 mg/mL, respectively, determined gravimetrically.

Hydrogels were obtained by the stepwise addition of $Cd(OAc)_2$ aqueous solution ($10^{-2}$ M) to the reprecipitated colloids or their mixtures up to complete gelation of the nanoparticles. The hydrogels were redissolved back into their colloidal form by the addition of an aliquot of $10^{-2}$ M ethylenediaminetetraacetic acid (EDTA) aqueous solution (adjusted to pH 12 by the addition of 1 M NaOH) equal to the $Cd^{2+}$ concentration in the gelated sample. The gelation process has been monitored directly in a 1 cm quartz cuvette by the stepwise addition of $Cd(OAc)_2$ solution into the diluted NC colloid (or colloid mixtures) with subsequent measurement of the absorbance, PL and PL lifetime. A critical point drier (13200J-AB from Spi Supplies) was used for supercritical $CO_2$ drying to prevent the fine nanostructures from collapsing and to obtain self-supporting aerogel monoliths. This drying technique is described in our previous work.[4c]

**Characterization.** UV−vis absorption spectra were recorded using a Cary 50 spectrophotometer (Varian Inc.). Absorption spectra from the aerogels were acquired on a Cary 5000 spectrophotometer (Varian Inc.) equipped with an Ulbricht sphere (Labsphere Varian) for measurements with scattering samples. **Fluorescence** measurements were performed with a FluoroMax-4 spectrofluorimeter (HORIBA Jobin Yvon Inc.). **Time resolved PL** traces were recorded on a Fluorolog-3 spectrofluorimeter (HORIBA Jobin Yvon Inc.) using a 200 ps pulsed laser diode emitting at 403 nm. All measurements were performed at room temperature. Prior to spectra measurements on aerogel samples, small pieces of them were placed between two quartz plates.

Samples for **transmission electron microscopy (TEM)** were prepared by dropping diluted aerogel dispersions, obtained by their quick sonication in methanol, onto copper grids coated with a thin Formvar-carbon film with subsequent evaporation of the solvent. TEM imaging was carried out on a Tecnai T20 microscope operating at 200 kV (FEI) and on a LIBRA microscope operating at 200 kV (Carl Zeiss AG). **Energy-dispersive X-ray spectroscopy (EDS)** and **scanning electron microscopy (SEM)** were performed on a Zeiss DSM 982 Gemini instrument. The samples for SEM and EDS characterization were prepared by deposition of the aerogel dispersions in methanol onto silicon slides with subsequent natural drying.

**Nitrogen physisorption** isotherms were measured at 77 K using an Autosorb 1 (Quantachrome). All samples were activated in vacuum at

**Scheme 1. Illustration of the Gelation Process of CdTe and Au NCs, Including Surface Exchange of Citrate with the 5-$HSCH_2$Tz Stabilizer for the Au Nanoparticles**
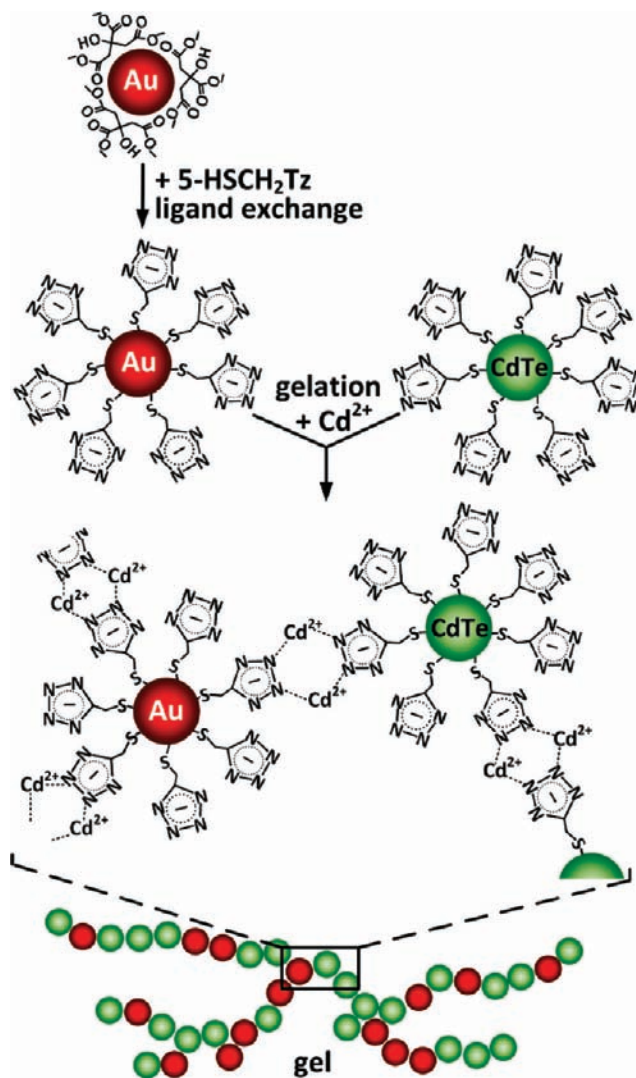


423 K for at least 24 h. The specific surface area was calculated using the Brunauer−Emmet−Teller (BET) equation ($p/p_0$ = 0.05−0.2). The pore volume was determined from the amount of adsorbed nitrogen at $p/p_0$ = 0.99. We note that using this method, only pores smaller than 200 nm are taken into consideration. The pore size distribution was estimated from the adsorption branch of the isotherm by using the BJH model.

## ■ RESULTS AND DISCUSSION

**Microscopy and Nitrogen Adsorption Characterization.** On the basis of our previously reported investigation of the synthesis and gelation of CdTe NCs capped by 5-$HSCH_2$Tz we have developed a new method for the preparation of hybrid aerogels composed of aqueous CdTe and Au nanoparticles. Both of these materials are stabilized with 5-$HSCH_2$Tz: CdTe by direct synthesis in the presence of the tetrazole, whereas gold particles originally capped by citrate underwent ligand exchange resulting in the replacement of the initially weakly bound citrate by the stronger binding mercaptomethyltetrazole. The latter
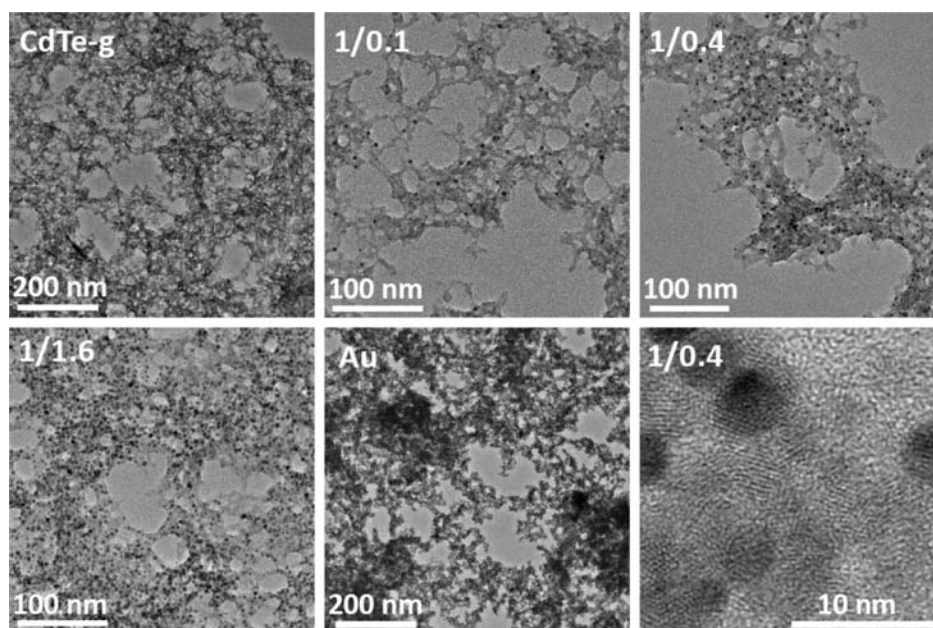
**Figure 1.** TEM images of fragments of pure CdTe-g, Au, and hybrid CdTe-g/Au aerogels of different compositions. The numbers shown are the CdTe-g/Au initial weight ratios. Bottom right: a high resolution TEM image of CdTe-g/Au (1/0.4) aerogel.

provides sufficiently higher stability for the gold colloid and enables its concentration and reprecipitation without notable aggregation of the particles. This similar coverage of both types of nanoparticles along with their similar average sizes (diameters of Au, CdTe-g and CdTe-o NCs are of about 3, 2, and 3 nm, respectively) ensures their similar stability, solubility and surface activity, which in turn results in a random distribution of the particles within the resulting 3D networks. The unique complexing ability of the tetrazole enables an efficient cross-linking of the particles via additional $Cd^{2+}$ ions (see Scheme 1).[8] Adding cadmium ions stepwise controls the level of aggregation of the NCs as will be shown below with the aid of optical spectroscopy.

Using two different CdTe NC fractions (CdTe-g and CdTe-o), we prepared two series of aerogels of different compositions, ranging from pure CdTe to pure Au. Our method allows the rapid gelation of the nanoparticles by addition of the appropriate amount of $Cd^{2+}$ ions. The method is easily up-scalable and does not involve any sophisticated processing like chemical destabilization of the initial colloid[4a,b] or its photochemical treatment reported earlier for the 3D assembly of CdTe NCs.[4c] For instance, immediate and complete gelation of pure CdTe NCs has been achieved by the addition of $10^{-2}$ M cadmium acetate water solution at a molar ratio of $Cd^{2+}$/CdTe NCs ≈ 50/1. Although a procedure for a determination of the CdTe concentration has been published by Yu et al.,[10] to the best of our knowledge there is no reliable method for the estimation of the Au particle concentration. Therefore, for the evaluation of the initial CdTe/Au ratios we used the weight concentrations of the NCs measured by gravimetry. It is worth mentioning that the concentration of the CdTe NCs calculated according to Yu et al. deviates considerably from that determined gravimetrically.

Besides the uniform distribution of the particles in the network, the equal capping enables an efficient control of its composition. As is clearly seen in Figure 1, showing TEM images of aerogels obtained from both individual CdTe-g and Au NCs, and their mixtures of different ratios, an increasing gold particle content in the initial NCs mixture leads to a corresponding increase of the Au content in the resulting hybrid aerogels. Note, owing to different contrasts in the TEM images, the Au particles appear as black dots, whereas the CdTe-g NCs are seen as continuous gray network. High resolution images reveal that this gray area consists of randomly oriented interconnected crystalline particles (see Figure 1, bottom right image). Images acquired by tilting the sample to 30 and 60° display that the gold particles are randomly distributed within the aerogel network in all three dimensions (see Figure SI1 in the Supporting Information, SI). In spite of their apparently tight binding, both CdTe and Au NCs maintain their nanosize properties (see below in the optical characterization). Nevertheless, cross-linking via complexing $Cd^{2+}$ ions withstands the drying of the hydrogels maintaining their high porosity. This porous structure on a larger scale is revealed by SEM imaging for all the samples obtained (see Figure SI2 in Supporting Information). According to our estimations based on volume and weight of the samples, the pure CdTe aerogels have a density of about 1/500th of that of bulk CdTe as reported earlier.[4c]

Table 1 shows the results of EDS elemental analysis of the hydrogels and the aerogels prepared from pure CdTe-o NCs, Au NCs, and their mixtures of different ratios. Although EDS does not allow for an exact quantification of the elemental content due to quite high instrumental errors, this technique provides useful information of a composition alteration. According to the EDS analysis, the CdTe-o NCs have a slightly higher tellurium content than the CdTe-g particles, and a strongly reduced sulfur content. The depletion of the S content indicates that during growth of the CdTe NCs, the stabilizer is partially lost due to its decomposition.

As follows from the table, the relative gold content in the hybrid hydro- and aerogels increases with increasing Au content in the initial mixture which, in addition to the TEM observations, confirms the tuneability of the network composition. The diminution of cadmium is accompanied by a decrease of the

**Table 1. Results of the Elemental Analysis (Performed by EDS) of the Initial CdTe NCs, the Pure CdTe-o, the Au and the Hybrid CdTe-o/Au Gels and Aerogels**

| sample (CdTe/Au initial wt. ratio) | state of the gel | relative molar content of elements | | | | CdTe/Au wt. ratio (EDS) |
|---|---|---|---|---|---|---|
| | | Cd | Au | Te | S | |
| initial CdTe-g NCs | colloid | 1 | | 0.42 | 1.32 | |
| initial CdTe-o NCs | colloid | 1 | | 0.48 | 0.58 | |
| Au pure | hydro | 0.14 | 1 | | 0.38 | |
| | aero | 0.13 | 1 | | 0.16 | |
| CdTe-o | hydro | 1 | | 0.4 | 0.6 | |
| | aero | 1 | | 0.43 | 0.64 | |
| 1/0.2 | hydro | 1 | 0.09 | 0.4 | 0.65 | 1/0.11 |
| | aero | 1 | 0.1 | 0.37 | 0.6 | 1/0.12 |
| 1/0.7 | hydro | 1 | 0.28 | 0.39 | 0.69 | 1/0.34 |
| | aero | 1 | 0.29 | 0.33 | 0.6 | 1/0.39 |
| 1/2.9 | hydro | 1 | 1.07 | 0.38 | 0.83 | 1/1.3 |
| | aero | 1 | 1.31 | 0.31 | 0.92 | 1/1.7 |

**Table 2. Surface Area and Pore Volume of the Pure CdTe-o, the Mixed CdTe/Au (1/1) and the Pure Au Aerogels**

| aerogel sample | surface area $[m^2/g]$ | pore volume $[cm^3/g]$ |
|---|---|---|
| CdTe-o | 80 | 0.18 |
| CdTe/Au (1/1) | 130 | 0.29 |
| Au | 50 | 0.51 |

tellurium and an increase of the sulfur contents. Although there are slight deviations between the relative elemental compositions of the hydrogels and the aerogels, the values obtained are in quite good agreement. In the resulting structure the gold content is lower than that estimated from the ratio of the NCs in the initial mixture due to the addition of extra $Cd^{2+}$ in the course of gelation. The same general trends were observed for the case of the CdTe-g colloid.

Further characterization of the aerogel samples has been carried out via nitrogen adsorption measurements that delivered information about their surface area, pore volume (presented in Table 2) and pore size distribution (shown in Figure 2). Although all isotherms acquired cannot be assigned to a special IUPAC standard isotherm, they are similar to type II (see Figure SI3 in Supporting Information). Especially the strong slope at a relative pressure of $p/p_0 > 0.95$, combined with the fact that the isotherm does not reach a saturation level clearly indicate the presence of a large amount of macropores. Moreover, a small hysteresis observed at $0.9 < p/p_0 < 0.99$ can be attributed to capillary condensation effects in the interparticular voids of the aerogels. Besides this, pure CdTe and mixed CdTe/Au (1/1) samples also exhibit a hysteresis at a relative pressure of $0.4 < p/p_0 < 0.8$ assigned to smaller pores in the mesopore range. This is clarified in the BJH pore size distribution showing mesopores in the range of 3−10 nm for CdTe and CdTe/Au samples (see Figure 2). In contrast to this, pure gold aerogel does not exhibit mesopores. The presence of smaller pores in the pure CdTe and CdTe/Au aerogels results in their larger surface areas (see Table 2). Since Au aerogel is almost purely macroporous, its specific surface area is smaller ($50\,m^2/g$), but at the same time the total pore volume is larger. If pores smaller than 200 nm are considered, then the Au aerogel exhibits with $0.51\,cm^3/g$ almost

twice the volume of the CdTe and hybrid aerogels ($0.18\,cm^3/g$ and $0.29\,cm^3/g$, respectively). We point out that the surface area and porosity of these materials depend not only on their structure and content but also on the conditions of the critical point drying. Incomplete drying may lead to the formation of denser areas (xerogellike structure) within the network affecting its whole surface area as well as the pore volume.

It is noted that the main purpose of the present work is to explore in detail the 3D-networking approach and to investigate the evolution of the optical properties of mixed gels and aerogels as a function of the gold content. That is why relatively less attention was paid to the strengthening of the aerogel structure.[11] Improvements of aerogel properties, including robustness, design of porosity, and additional modification by functional molecules or polymers will be the topic of a forthcoming publication.

**Optical Characterization.** PL and absorption spectra of the initial colloids used for assembly are presented in Figure 3. As is seen from the figure, the CdTe samples have been chosen so that the emission of the sample CdTe-g overlaps the plasmon resonance maximum of the gold nanoparticles, whereas the orange emission of CdTe-o is located at longer wavelengths. We note that after ligand exchange the gold plasmon resonance is shifted by approx 11 nm to longer wavelengths most probably due to the difference in the electron donating properties of citrate and $5\text{-}HSCH_2Tz$ (better donor) having influence on the free electron density of the Au particles.[12]

In Figure 4 are displayed the optical properties of the pure CdTe-g and Au colloids as well as their mixtures in the course of their gelation by means of PL, absorbance as well as by time-resolved PL spectroscopy. Analyzing the results certain trends for all of the systems investigated are observed. The addition of $Cd^{2+}$ leads to the appearance of scattering seen clearly in the absorbance spectra due to NC aggregate formation. We note that the spectra of the mixtures are superpositions of the absorbance of the semiconductor particles and the metal plasmon resonance. In all cases, the degree of aggregation is controllable by the amount of metal ions added until ultimately all the particles in solution are connected into a 3D network. The positions of the absorbance maxima of the pure CdTe colloid and the CdTe/Au mixtures with low gold content are virtually unaltered. The
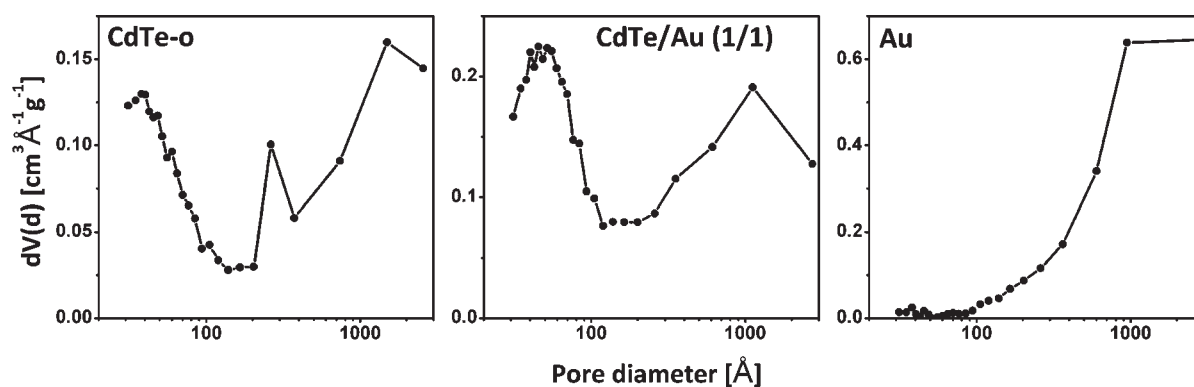
**Figure 2.** Pore size distribution of the pure CdTe-o, the hybrid CdTe/Au (1/1) and the pure Au aerogels from BJH theory determined from the adsorption branch of the isotherms.
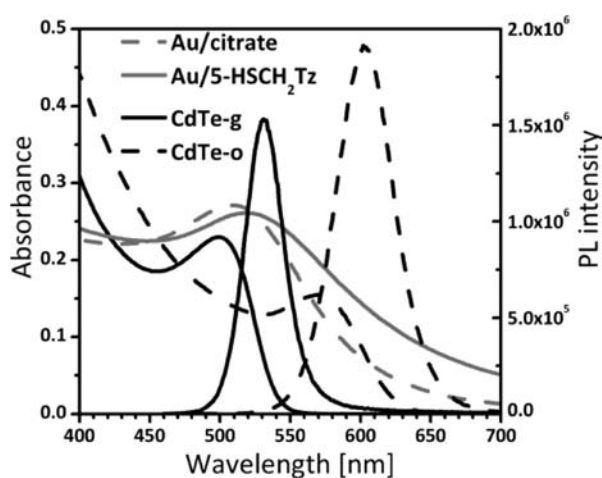


**Figure 3.** PL ($\lambda_{ex.}$ = 450 nm) and absorption spectra of the initial CdTe-g and CdTe-o NCs colloids, and absorbance spectra of the Au/citrate and Au/5-HSCH$_2$Tz NCs obtained after ligand exchange.

addition of larger amounts of gold colloid, resulting in a dominant plasmon peak in the absorbance spectra, leads to a shift of the position of this maximum to longer wavelengths during gelation. This is seen even more clearly in the case of the pure gold colloid: a distinct broadening of the gold plasmon band and its shift to longer wavelength originates from the interaction of the particles being in close proximity or even partly fused. A similar behavior of gold plasmon has been reported recently for Au NPs assembled in a film by layer-by-layer deposition.[13] Nevertheless, according to the shape of the spectra it is obvious that even being interconnected into a 3D network, the Au NCs retain their properties as individual units. For all of the samples investigated, a degelation is possible by the addition of EDTA due to its stronger complexation ability toward Cd ions than 5-HSCH$_2$Tz, as it was shown earlier for pure CdTe NCs.[8]

The next general observation concerns the PL quenching of both pure CdTe and its mixtures with Au NCs. On the one hand, the assembly of the CdTe NCs leads to the appearance of additional channels for nonradiative deactivation through fast energy transfer analogous to that in clusters of CdTe NCs electrostatically bound by Ca$^{2+}$.[14] The proximity of the nanoparticles incorporated into the network allows for both Förster and Dexter energy transfer mechanisms. An additional reduction

of the emission lifetime by gelation of the NCs could be induced by enhanced energy transfer from originally luminescent quantum dots to "dark" ones which are commonly present in NC ensembles.[15] However, in the case of the hybrid structures an additional decrease in the PL is imposed by the gold nanoparticles which are well-known as efficient quenchers of the emission of CdTe NCs.[16] Thus, by steady state PL measurements on the green CdTe we observed a remaining 9% of the initial emission intensity for the pure CdTe-g sample upon full gelation via Cd$^{2+}$. In the three mixtures CdTe-g/Au = 1/0.1, 1/0.4 and 1/1.6, the residual emission intensity of 15, 35 and 10% was observed, respectively. Consequently, we may assume that at relatively low gold content the quenching occurs mostly through the nonradiative energy transfer within the semiconductor network. A decreased quenching with increasing gold content implies that in this case the Au particles act as separators between the CdTe units partially preventing the formation of energy drain channels. An additional increase in the emission relative to the pure CdTe gel in the case of the 1/0.1 and 1/0.4 hybrids of 6 and 26%, respectively, can be attributed to a plasmon-enhanced emission frequently reported for metal-emitting entity interfaces.[13,17] Therefore, in the hybrid system, the gold NCs simultaneously play roles of emission quenchers, separators, and emission enhancers, resulting in a certain balance between quenching and enhancement depending on the content of gold particles. The enhancement observed is not very efficient due to the absence of a well-controlled spacer between the plasmonic and the emitting blocks of the structure. The introduction of such spacers, e.g., in the form of a dielectric shell on the gold particle core, is foreseen as an optional solution here. However, at a given point the Au NCs change their role and constitute the main contribution to the emission degradation of the system. The PL quenching may be attributed to electron transfer from the orbitals below the Fermi level of gold, as reported by Nikoobakht et al. for CdSe NCs showing trap-related luminescence.[18] In the case of CdTe, the strong band gap emission is quenched most probably by nonradiative recombination of electrons from the Au and holes of the excited CdTe particles or oppositely, through capturing exited electron of the semiconductor by the gold particle, depending on the relative positions of the semiconductor band gap and Fermi level of gold. At the same time, a contribution of the gold NCs to quenching through Förster energy transfer is also possible.[16,19]
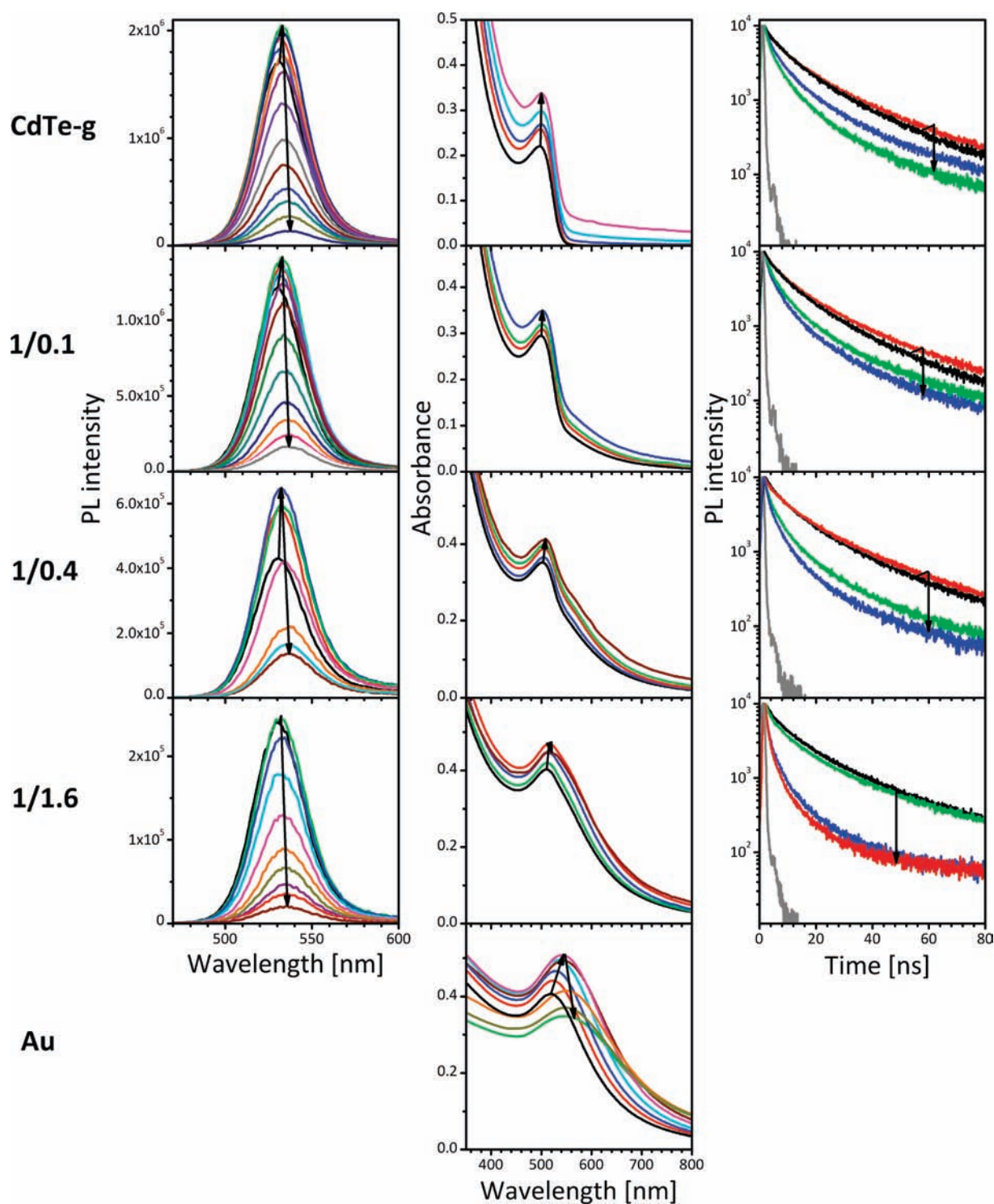
**Figure 4.** Evolution of PL ($\lambda_{ex.}$ = 450 nm), absorbance and time-resolved PL ($\lambda_{ex.}$ = 403 nm) of CdTe-g and mixed CdTe-g/Au colloids, and absorbance of the Au colloid during their gelation by the addition of $Cd^{2+}$ ions. The numbers shown on the left are the CdTe-g/Au initial weight ratios. The arrows indicate increasing $Cd^{2+}$ concentration.

The PL quenching during the gelation is accompanied by a shift of the luminescence maximum of about 7 nm to longer wavelengths for all of the samples. Most probably this is due to energy transfer from smaller NCs (donors) to larger ones (acceptors), as also suggested by the PL lifetime measurements (see Figure 4). It is clearly seen that the luminescence of the aggregated NCs decays much faster than that of the initial colloid (photoluminescence lifetime parameters of the CdTe-g NCs in the course of their gelation in the mixture with Au nanoparticles are summarized in Table SI1 in the Supporting Information).

Moreover, an increase of the gold content in the assembly supplementary diminishes the PL lifetime of the CdTe confirming
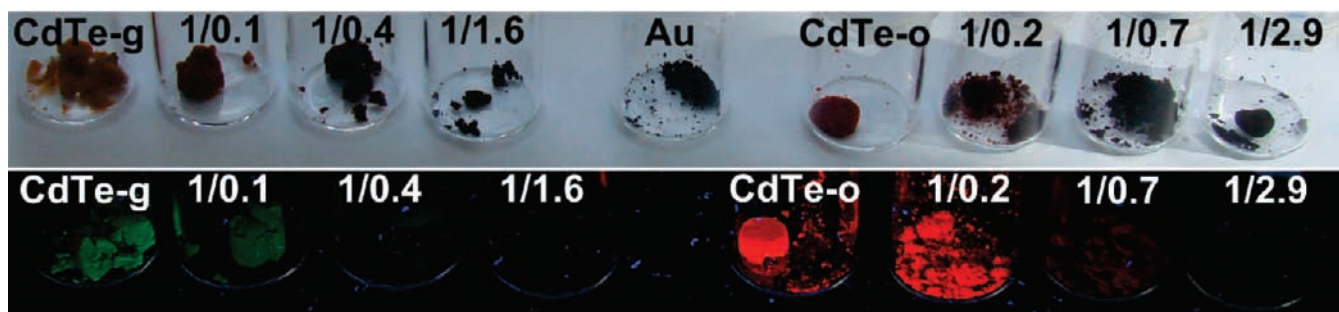
**Figure 5.** Photographs of pure CdTe, Au, and hybrid CdTe/Au aerogels of different compositions under day (top) and UV (365 nm) light (bottom). The numbers shown are the CdTe/Au initial weight ratios. Some gels were partly destroyed during postpreparative handling necessary for their characterization.
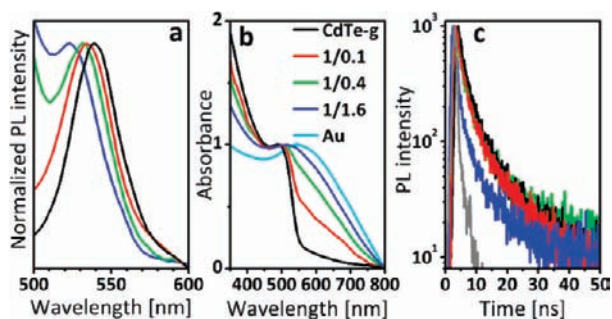


**Figure 6.** PL ($\lambda_{ex.}$ = 450 nm) (a), absorbance (b) and PL lifetime ($\lambda_{ex.}$ = 403 nm) (c) of pure CdTe-g, Au (absorbance only) and hybrid CdTe-g/Au aerogels. The numbers shown are the CdTe-g/Au initial weight ratios. Note, the shoulders in the PL spectra of the 1/0.4 and 1/1.6 aerogels (a) at short wavelengths are due to reflexions of the excitation beam from quartz plate, which dominate the emission of the samples due to its low intensity.

that Au NCs effectively increase emission decay rate. Interestingly, by the addition of the first aliquots of cadmium acetate solution the PL intensity as well as its lifetime enhance (see Figure 4) implying a reconstruction of the CdTe surface and the elimination of trap states analogous to the process reported by Gao et al.[20] Photographs of two series of aerogels (with green and orange CdTe NCs) prepared from the corresponding hydrogels visually demonstrate the difference in luminescence depending on the composition of the system (see Figure 5). Increasing gold content leads to efficient quenching of the luminescence of the CdTe NCs of both sizes. Here we note that all trends observed by spectroscopy and discussed above for the green emitting CdTe sample are observed also for the orange emitting sample. A similar optical behavior is displayed by gelating NCs in the presence of other cations as e.g. $Zn^{2+}$, $Ba^{2+}$, $Ni^{2+}$ (shown in Figure SI4 of the Supporting Information). In these cases, an enhancement of the emission properties of CdTe NCs after addition of the first portions of the salt solutions has not been observed since the cations used do not eliminate surface traps from the nanoparticles. The addition of $Ni^{2+}$ resulted in almost complete PL quenching most probably due to strong interactions with the surface of the CdTe particles leading to the formation of additional surface traps.

Figure 6 shows PL, absorbance and luminescence lifetime measurements of the aerogels prepared employing CdTe-g and Au colloids. Comparing the optical properties of the initial NC colloid and the aerogels, we clearly see a strong red shift of the PL

for the pure CdTe sample, while its absorption maximum is slightly shifted to shorter wavelengths. This observation may be explained by a partial fusion of the NCs during the gelation and especially by subsequent drying of the resulting assemblies, which leads to a decrease in the extent of quantum confinement and an overlap of the wave functions of the nanoparticles. This induces a further decrease of the emission lifetime relative to the hydrogel state (cf. Figure 6c and 4, see also Table SI1). The presence of the gold particles results in a blue shift of the luminescence maximum of the aerogels, approaching that of the initial NCs with increasing gold content. Probably, in this case, the Au particles act as spacers between the CdTe NCs preventing their fusion. Although the absorption of the aerogels containing a large amount of Au particles is dominated by the gold plasmon resonance, the two first hybrid samples (with a ratio of CdTe-g/Au = 1/0.1 and 1/0.4, CdTe-o = 1/0.2 and 1/0.7 (not shown)) exhibit a slight red shift for the green CdTe particles and almost no alterations with regard to the maxima of the CdTe-o particles. This distinct shift of the absorbance maxima of the CdTe NCs with increasing gold content in the assembly most probably is due to an alteration of the quantum confinement owing to a change of the local surrounding of the nanoparticles.

## ■ CONCLUSIONS

A new approach is presented for a facile and reproducible preparation of 3D assemblies of colloidal nanoparticles. The networking of the NCs occurs via cadmium ion complexation with the tetrazolate ligands on the surface of both, CdTe and Au nanocrystals in aqueous media. Apart from $Cd^{2+}$, other ions of less toxic metals like Zn, Ba, Ni, Ag, or Au are applicable for the assembly. The equal capping of both types of nanocrystals ensures the formation of hybrid semiconductor-metal gel-like structures with tunable composition. The gelation process has been monitored by means of photoluminescence, absorption, and emission lifetime spectroscopy. The resulting assemblies processed by critical point drying form highly porous aerogels with the surface area in the range of 50−130 $m^2$/g and the pore volume of 0.18−0.51 $cm^3$/g. Optical studies have shown a distinct dependence of the optical properties of the 3D hydro- and aerogels on their composition. Gelation and the increase of the gold content in the hybrid architectures induce luminescence quenching and shortening of the emission lifetime. The method developed is promising for biological and chemical beacon measurements: optical detection of molecules interacting with

metal and/or semiconductor nanoparticles in highly porous nanostructures. The structures obtained require further investigation, especially in terms of their energy and charge transporting properties, as well as of their proper design aiming at their application in electronics, nanophotonics and photovoltaics.

## ■ ASSOCIATED CONTENT

**ⓢ  Supporting Information.**   SEM images of pure CdTe-g, Au, and hybrid CdTe-g/Au aerogels of different compositions; TEM images of CdTe-g/Au (1/0.4) aerogel acquired by tilting to 30 and 60°; nitrogen physisorption isotherms of the pure CdTe-o, the hybrid CdTe/Au (1/1) and the pure Au aerogels; table of photoluminescence lifetime parameters of the CdTe-g NCs in the course of their gelation in the mixture with Au nanoparticles as well as those of the aerogel samples; evolution of the PL, absorbance and time-resolved PL of CdTe-g and mixed CdTe-g/Au colloids during their gelation by the addition of $Zn^{2+}$, $Ba^{2+}$, $Ni^{2+}$ ions. This material is available free of charge via the Internet at http://pubs. acs.org.

## ■ AUTHOR INFORMATION

**Corresponding Author**
alexander.eychmueller@chemie.tu-dresden.de.

## ■ ACKNOWLEDGMENT

## ■ REFERENCES

(1) (a) Rogach, A. L.; Talapin, D. V.; Shevchenko, E. V.; Kornowski, A.; Haase, M.; Weller, H. *Adv. Funct. Mater.* **2002**, *12*, 653. (b) Talapin, D. V.; Lee, J.-S.; Kovalenko, M. V.; Shevchenko, E. V. *Chem. Rev.* **2010**, *110*, 389–458.

(2) Gaponik, N. *J. Mater. Chem.* **2010**, *20*, 5174–5181.

(3) Wessels, J. M.; Nothofer, H.-G.; Ford, W. E.; von Wrochem, F.; Scholz, F.; Vossmeyer, T.; Schroedter, A.; Weller, H.; Yasuda, A. *J. Am. Chem. Soc.* **2004**, *126*, 3349–3356.

(4) (a) Mohanan, J. L.; Arachchige, I. U.; Brock, S. L. *Science* **2005**, *307*, 397–400. (b) Arachchige, I. U.; Brock, S. L. *Acc. Chem. Res.* **2007**, *40*, 801–809. (c) Gaponik, N.; Wolf, A.; Marx, R.; Lesnyak, V.; Schilling, K.; Eychmüller, A. *Adv. Mater.* **2008**, *20*, 4257–4262.

(5) Bag, S.; Trikalitis, P. N.; Chupas, P. J.; Armatas, G. S.; Kanatzidis, M. G. *Science* **2007**, *317*, 490–493.

(6) Chen, H.; Lesnyak, V.; Bigall, N. C.; Gaponik, N.; Eychmüller, A. *Chem. Mater.* **2010**, *22*, 2309–2314.

(7) (a) Bigall, N. C.; Herrmann, A.-K.; Vogel, M.; Rose, M.; Simon, P.; Carrillo-Cabrera, W.; Dorfs, D.; Kaskel, S.; Gaponik, N.; Eychmüller, A. *Angew. Chem.-Int. Ed.* **2009**, *48*, 9731–9734. (b) Leventis, N.; Chandrasekaran, N.; Sadekar, A. G.; Mulik, S.; Sotiriou-Leventis, C. *J. Mater. Chem.* **2010**, *20*, 7456–7471. (c) Tappan, B. C.; Huynh, M. H.; Hiskey, M. A.; Chavez, D. E.; Luther, E. P.; Mang, J. T.; Son, S. F. *J. Am. Chem. Soc.* **2006**, *128*, 6589–6594.

(8) Lesnyak, V.; Voitekhovich, S. V.; Gaponik, P. N.; Gaponik, N.; Eychmüller, A. *ACS Nano* **2010**, *4*, 4090–4096.

(9) Brown, K. R.; Walter, D. G.; Natan, M. J. *Chem. Mater.* **2000**, *12*, 306–313.

(10) Yu, W. W.; Qu, L.; Guo, W.; Peng, X. *Chem. Mater.* **2003**, *15*, 2854–2860.

(11) (a) Hüsing, N.; Schubert, U. *Angew. Chem.-Int. Ed.* **1998**, *37*, 22–45. (b) Leventis, N. *Acc. Chem. Res.* **2007**, *40*, 874–884.

(12) (a) Mulvaney, P. *Langmuir* **1996**, *12*, 788–800. (b) Alvarez, M. M.; Khoury, J. T.; Schaaff, T. G.; Shafigullin, M. N.; Vezmar, I.; Whetten, R. L. *J. Phys. Chem. B* **1997**, *101*, 3706–3712.

(13) Ozel, T.; Nizamoglu, S.; Sefunc, M. A.; Samarskaya, O.; Ozel, I. O.; Mutlugun, E.; Lesnyak, V.; Gaponik, N.; Eychmüller, A.; Gaponenko, S. V.; Demir, H. V. *ACS Nano* **2011**, *5*, 1328–1334.

(14) Mayilo, S.; Hilhorst, J.; Susha, A. S.; Höhl, C.; Franzl, T.; Klar, T. A.; Rogach, A. L.; Feldmann, J. *J. Phys. Chem. C* **2008**, *112*, 14589–14594.

(15) Ebenstein, Y.; Mokari, T.; Banin, U. *Appl. Phys. Lett.* **2002**, *80*, 4033–4035.

(16) Zhang, J.; Badugu, R.; Lakowicz, J. R. *Plasmonics* **2008**, *3*, 3–11.

(17) (a) Komarala, V. K.; Rakovich, Y. P.; Bradley, A. L.; Byrne, S. J.; Gun'ko, Y. K.; Gaponik, N.; Eychmüller, A. *Appl. Phys. Lett.* **2006**, *89*, 253188. (b) Okamoto, K.; Vyawahare, S.; Scherer, A., *J. Opt. Soc. Am. B* **2006**, *23*, 1674–1678. (c) Curto, A. G.; Volpe, G.; Taminiau, T. H.; Kreuzer, M. P.; Quidant, R.; van Hulst, N. F. *Science* **2010**, *329*, 930–933. (d) Song, J. H.; Atay, T.; Shi, S.; Urabe, H.; Nurmikko, A. V. *Nano Lett.* **2005**, *5*, 1557–1561. (e) Kulakovich, O.; Strekal, N.; Yaroshevich, A.; Maskevich, S.; Gaponenko, S.; Nabiev, I.; Woggon, U.; Artemyev, M. *Nano Lett.* **2002**, *2*, 1449–1452. (f) Ray, K.; Badugu, R.; Lakowicz, J. R. *J. Am. Chem. Soc.* **2006**, *128*, 8998–8999. (g) Shimizu, K. T.; Woo, W. K.; Fisher, B. R.; Eisler, H. J.; Bawendi, M. G. *Phys. Rev. Lett.* **2002**, *89*, 117401. (h) Ozel, T.; Soganci, I. M.; Nizamoglu, S.; Huyal, I. O.; Mutlugun, E.; Sapra, S.; Gaponik, N.; Eychmüller, A.; Demir, H. V. *New J. Phys.* **2008**, *10*, 083035. (i) Lunz, M.; Gerard, V. A.; Gun'Ko, Y.; Lesnyak, V.; Gaponik, N.; Susha, A.; Rogach, A. L.; Bradley, A. L. *Nano Lett.* DOI: 10.1021/nl201714y.

(18) Nikoobakht, B.; Burda, C.; Braun, M.; Hun, M.; El-Sayed, M. A. *Photochem. Photobiol.* **2002**, *75*, 591–597.

(19) (a) Huang, T.; Murray, R. W. *Langmuir* **2002**, *18*, 7077–7081. (b) Wargnier, R.; Baranov, A. V.; Maslov, V. G.; Stsiapura, V.; Artemyev, M.; Pluot, M.; Sukhanova, A.; Nabiev, I. *Nano Lett.* **2004**, *4*, 451–457.

(20) Gao, M.; Kirstein, S.; Möhwald, H.; Rogach, A. L.; Kornowski, A.; Eychmüller, A.; Weller, H. *J. Phys. Chem. B* **1998**, *102*, 8360–8363.